

Relationship of central incisor implant to the ridge configuration anterior to the nasopalatine canal in dentulous and partial edentulous individuals: A comparative study

Xueting Jia, Wenjie Hu, Huanxin Meng

Background: The aims of this study were to investigate the contour alteration of the ridge anterior to the nasopalatine canal after tooth loss and the difference between the incidences of the nasopalatine canal perforation in dentulous and edentulous patients by cone-beam computed tomography. **Methods:** 72 cone-beam computed tomography scans were selected from database. In 36 subjects of them, both maxillary central incisor were present, while the rest were edentulous ridges missing one maxillary central incisor. The configuration of the ridge anterior to the canal were recorded, including lingual concavity depth, lingual concavity height, lingual concavity angle, bone height coronal to the incisive foramen, and bone width anterior to the canal. The incidence of perforation were evaluated after implant placement in the cingulum position with the long axis following that of its restoration on images. **Results:** Comparing with variable values in dentulous patients, the lingual concavity depth and angle were greater by 0.9 mm and 4°, and bone height was shorter by 1.1 mm in edentulous patients, respectively. Besides, bone width in edentulous patients was narrower than in dentulous patients by 1.2 mm at incisive foramen level and 0.9 mm at 8 mm subcrestal level, respectively. After 72 virtual cylindrical implants (4.1 × 12 mm) were placed, a total of 12 sites (16.7%) showed a perforation and three-fourths occurred in edentulous patients. After replacing with 72 tapered implants (4.3 × 13 mm), a total of 6 implants (8.3%) broke into the canal, which all belonged to edentulous patients. **Conclusions:** The nasopalatine canal may get close to the implant region after the central incisor extraction, and the bone width anterior to the canal may also reduce. The perforations may occur more commonly in edentulous patients.

1 **Relationship of central incisor implant to the ridge configuration anterior to the**
2 **nasopalatine canal in dentulous and partial edentulous individuals: A comparative study**

3
4 **Abstract**

5 Background: The aims of this study were to investigate the contour alteration of the ridge anterior
6 to the nasopalatine canal after tooth loss and the difference between the incidences of the
7 nasopalatine canal perforation in dentulous and edentulous patients by cone-beam computed
8 tomography.

9 Methods: 72 cone-beam computed tomography scans were selected from database. In 36 subjects
10 of them, both maxillary central incisor were present, while the rest were edentulous ridges missing
11 one maxillary central incisor. The configuration of the ridge anterior to the canal were recorded,
12 including lingual concavity depth, lingual concavity height, lingual concavity angle, bone height
13 coronal to the incisive foramen, and bone width anterior to the canal. The incidence of perforation
14 were evaluated after implant placement in the cingulum position with the long axis following that
15 of its restoration on images.

16 Results: Comparing with variable values in dentulous patients, the lingual concavity depth and
17 angle were greater by 0.9 mm and 4°, and bone height was shorter by 1.1 mm in edentulous
18 patients, respectively. Besides, bone width in edentulous patients was narrower than in dentulous
19 patients by 1.2 mm at incisive foramen level and 0.9 mm at 8 mm subcrestal level, respectively.

20 After 72 virtual cylindric Implants (4.1 × 12 mm) were placed, a total of 12 sites (16.7%) showed
21 a perforation and three-fourths occurred in edentulous patients. After replacing with 72 tapered

22 implants (4.3×13 mm), a total of 6 implants (8.3%) broke into the canal, which all belonged to
23 edentulous patients.

24 Conclusions: The nasopalatine canal may get close to the implant region after the central incisor
25 extraction, and the bone width anterior to the canal may also reduce. The perforations may occur
26 more commonly in edentulous patients.

27

28 Keywords: alveolar bone, anterior maxilla, cone-beam computed tomography, dental implants,
29 nasopalatine canal

30

31 **List of authors:**

32 Xueting Jia[#], Wenjie Hu[#], Huanxin Meng^{*}

33 Department of Periodontology, Peking University School and Hospital of Stomatology, Beijing,
34 China

35 [#] These authors contributed equally to this work and should be considered co-first authors.

36 *** Corresponding author**

37 Huanxin Meng

38 Department of Periodontology, Peking University School and Hospital of Stomatology

39 22 S Zhongguancun Ave,

40 Haidian District, Beijing, China 100081

41 Tel: (8610) 82195368 Fax: (8610) 62173402

42 E-mail: kqhxmeng@bjmu.edu.cn; kqhxmeng@126.com

43 **Introduction**

44 Dental implant restoration has become a very common treatment in dental practices.¹⁻³ In the
45 esthetic zone, the primary goal of implant treatment is to re-establish both esthetics and function.⁴
46 As generally accepted, the implant placement is supposed to be based on a restorative-driven
47 philosophy.⁵ According to this concept, the three-dimensional ideal implant position has been
48 described.⁶⁻¹⁰ Mesiodistally, a single implant should be no closer than 1.5 mm away from adjacent
49 root surface. Apicocoronally, the implant platform is supposed to be placed 2 to 4 mm apical to
50 the expected midfacial gingival margin. Buccolingually, the implant should be positioned slightly
51 palatal to the incisal edge and 2 mm of buccal bone is recommended. With regard to the implant
52 axis, in order to use a prefabricated abutment and a screw-retained crown, and to avoid excessive
53 off-axis loading, placement of an implant axis in alignment with the crown is recommended.¹¹

54 However, in both implant and delayed implant therapy, the nasopalatine canal (NPC) is often
55 an anatomical limitation for a maxillary central incisor implant placement in an ideal position
56 according to the restorative-driven philosophy. The NPC is a bony channel located posterior to the
57 maxillary central incisors and connects the nasal floor with the oral cavity. The NPC contains the
58 nasopalatine nerve and the terminal branch of descending nasopalatine artery, as well as fibrous
59 connective tissue, fat, and even small salivary glands.^{12,13} The relative location of NPC in the
60 maxilla was usually described by assessing the dimension of the buccal bone plate anterior to this
61 canal in many studies, and a closer proximity of NPC to the implant surgical site after tooth
62 extraction has been reported.¹⁴⁻¹⁶ Insertion of implants into the NPC may lead to contact of
63 implants with connective tissue and cause non-osseointegration¹⁷ or nasopalatine duct cyst.¹⁸⁻²⁰

64 Kraut & Boyden reported that the likelihood of finding a nasopalatine canal of a size that will
65 be detrimental to the placement of dental implants was approximately 4% by evaluating the
66 volumes of the NPC and bone anterior to the canal in CBCT images of 30 American patients.²¹
67 However, the incidence of perforation into the NPC is associated with not only the anatomic
68 morphology, but also the feature of the implant and the three-dimensional implant position.
69 Although the relative location of the central incisor implant and the NPC was very important, the
70 incidence of perforation into the NPC when a central incisor implant is placed in an ideal position
71 following an optimal axis was not well known yet. In addition, whether the change of the ridge
72 morphology caused by tooth loss will increase the incidence of perforation has not been assessed.
73 Besides, the feature of the exposure and the risk factors of the perforation have never been
74 analyzed. Whether a tapered implant or a minor adjustment of implant angulation could be
75 beneficial for avoidance of perforation was also not well known.

76 Cone-beam computed tomography (CBCT) has been widely used in clinical evaluation before
77 implant surgery because of the capability of accurate three-dimension imaging.²² Moreover, virtual
78 implant placement in CBCT images could provide an overall evaluation of implant position, as
79 well as the proximity of the implant to the anatomic structure.^{23,24} Therefore, the aims of this study
80 are to investigate the contour alteration of the ridge anterior to the nasopalatine canal after tooth
81 loss and the difference between the incidences of the nasopalatine canal perforation in dentulous
82 and edentulous patients by cone-beam computed tomography.

83

84 **Materials and Methods**

85

86 **Patient Selection**

87 This study was approved by the Biomedical Ethics Committee of Peking University School
88 of Stomatology (approval ID PKUSSIRB-201519006). The pre-existing CBCT data (Vatech CT,
89 Korea) selected for this study were performed from January 2011 to July 2014 for treatment
90 planning of implant procedures. Appropriate methodology and sample size were determined by a
91 pilot study and power analysis. It was determined that a sample of 36 specimens per group (for a
92 total sample of 72) was needed to represent a clinically significant difference in bone width anterior
93 to the nasopalatine canal. The sample size was calculated with $\alpha = 0.05$ and power = 0.90.

94 Images selected for this study had to fulfill the following inclusion criteria: (1) Chinese adults;
95 (2) clear view without scattering artifacts; (3) complete image of the NPC; (4) all six maxillary
96 anterior teeth were present or only one maxillary central incisor and at least one pair of maxillary
97 lateral incisors or one pair of maxillary canines were present; (5) the present maxillary anterior
98 teeth without obvious crowding or spacing; (6) no deep overbite or deep overjet in the anterior
99 teeth area; (7) at least two pairs of posterior teeth which could be retained with occlusal contact on
100 each side. Images were excluded if: (1) both maxillary central incisor were present but the amount
101 of alveolar bone loss exceeded one third of root length; (2) unhealed extraction sockets; (3) bone
102 graft material was present in the images; (4) both maxillary central incisors were missing; (5)
103 alveolar ridge height of implant region was less than 14 mm or the ridge width was less than 3.5
104 mm at the level of 2 mm below the bone crest. Images were categorized into two groups according
105 to dental status. That all maxillary anterior teeth were present was classified as dentulous group,

106 while the edentulous ridge missing one maxillary central incisor was classified as edentulous
107 group. The distributions of age, gender, NPC shape¹⁵ on sagittal slice and implant site were well
108 matched between two groups, respectively.

109

110 **Data Reconstruction**

111 All images were obtained using a CBCT machine (Vatech CT, Korea) in the Peking
112 University School of Stomatology by experienced radiologists. The imaging parameters were set
113 at 90 kVp, 7.0 mAs, scan time 24 seconds, resolution 0.15 mm and a field of view that varied
114 based on the region scanned. The scans included in this study were selected from the database and
115 processed with a measurement software program (Ez3D2009 Premium Ver. 1.2.1.0) in a
116 password-protected computer. The observer filtered CBCT images using Liquid Crystal Display
117 at a $1,280 \times 1,024$ screen resolution under room lighting. The distance between display and the
118 observer was 30 cm approximately. The scans were reoriented so that the maxilla was bilaterally
119 symmetric and the long axis of the sagittal CBCT slice was determined following the long axis of
120 the crown (connecting the buccolingual midpoint at the cemento-enamel junction and the point at
121 the incisal edge) of the maxillary central incisor. The data were reconstructed with slices at an
122 interval of 0.5 mm. The luminance and grayscale were adjusted to obtain clear CBCT views.

123

124 **Configuration of Ridge Anterior to the NPC**

125 The lingual concavity of the alveolar ridge anterior to the NPC was analyzed by observing
126 the sagittal slices (Fig 1 A) and measuring:

127 (1) The lingual concavity depth (LCD), the distance between the deepest point of the buccal
128 plate on the lingual side and a reference line parallel to the sagittal long axis of the central incisor
129 crown and passing through the labial opening of incisive foramen.

130 (2) The lingual concavity height (LCH), the distance between the deepest point of the buccal
131 plate on the lingual side and a reference line perpendicular to the sagittal long axis of the central
132 incisor crown and passing through the alveolar bone crest.

133 (3) The lingual concavity angulation (LCA), the angulation between the line connecting the
134 deepest point of the lingual concavity and the labial opening of incisive foramen and the line
135 parallel to the long axis of the central incisor crown and passing through the deepest point of the
136 lingual concavity.

137 Subsequently, the height of the alveolar bone coronal to the NPC (BH) was also recorded by
138 measuring the vertical distance between the alveolar bone crest and the line perpendicular to the
139 sagittal long axis of the central incisor crown and passing through the labial opening of incisive
140 foramen in the midsagittal plane of the NPC (Fig 1 A).

141 In addition, the minimum width of buccal bone plate anterior to the NPC (BW) was measured
142 in the axial view images at three levels: incisive foramen level, 8 mm subcrestal level and 14 mm
143 subcrestal level (Fig 1 B).

144

145 **Relative Location of the NPC and the Virtual Implant**

146 72 Cylindric implants (Straumann Bone-Level Implant, 4.1×12 mm) and 72 tapered implants
147 (Nobel Replace Select Tapered Implant 4.3×13 mm) were placed virtually in the selected

148 maxillary central incisor sites sequentially.

149 In the dentulous group, each implant was placed in the midsagittal plane of selected maxillary
150 central incisor mesiodistally. Buccolingually, the most lingual point of the implant platform was
151 located at that of the cingulum of this central incisor. Apicocoronally, the implant platform was
152 placed 2 mm below the crestal level. The sagittal long axis of the implant was parallel to that of
153 the central incisor crown (Fig 2 A-C).

154 In the edentulous group, each implant was placed in the center of the edentulous site
155 mesiodistally. Buccolingually, the implant platform was also placed at the cingulum position.¹¹
156 The details were present as follows: connecting the most prominent points of the two lateral
157 incisors or the two canines on their lingual side to draw a reference line and measuring the distance
158 between the cingulum of the natural contralateral central incisor at its most lingual point and the
159 reference line, and then the most lingual point of the implant platform was placed labial to the
160 reference line by the same distance. Apicocoronally, the location of the implant platform was the
161 same as that of the dentulous group. The sagittal long axis of the implant was parallel to that of the
162 contralateral central incisor crown (Fig 2 D-F).

163 After each virtual implant was placed, whether the implant broke through the interior wall of
164 the NPC was assessed in the sagittal and axial views slice by slice. For the NPC perforation cases
165 caused by cylindrical implants, the position of the implant platform was kept unchanged and the
166 embedded direction was rotated distally and labially by a minor angulation (5° and 10°),
167 respectively. The size and the location of each perforation were measured in the sagittal and axial
168 view images, which included its length, depth, area and the distance between the most coronal

169 point of the perforation and the alveolar bone crest.

170 All measurements were conducted by two examiners. The inter- and intraexaminer agreement
171 was determined by comparing two repeated measurements at 20 randomly chosen sites taken 1
172 week apart.

173

174 **Statistical Analysis**

175 All statistical analysis was performed using a statistical package (IBM, SPSS Statistics 19.0).
176 The inter- and intraexaminer agreement was determined using a t test. All measurements were
177 presented as means \pm standard deviations (SDs). The occurrence of the NPC perforation was
178 expressed as the number of sites and the percentage of the number of sites divided by the total
179 number of sites. The LCD, LCH, LCA, BH and BW were compared between dentulous group and
180 edentulous group by Mann-Whitney U test. The chi-square test was used to compare the incidences
181 of perforation between groups, genders and sides. Univariate and multivariate logistic regression
182 analyses were performed to identify risk factors associated with the NPC perforation. The
183 significance level (P value) was set at 0.05.

184

185 **Results**

186

187 A total of 703 subjects were screened and 72 subjects (54 males and 18 females) were selected
188 for this study. The mean age was 45.6 years, with a range of 28 to 64. Each group consisted of 36
189 subjects. The age, gender and implant site were well matched between the dentulous group and

190 the edentulous group, respectively. The distribution of NPC shape recorded on sagittal plane did
191 not show statistically significant differences between groups (Table 1). The intraexaminer and
192 interexaminer agreements were 0.94 and 0.87, respectively.

193 Table 2 illustrated the measuring results of configuration of ridge anterior to the NPC. A total
194 of 54 ridges (75.0%) showed a lingual concavity in sagittal views. The mean LCD, LCH and LCA
195 values were 1.8 ± 1.7 mm, 14.3 ± 7.3 mm and $8.6 \pm 6.5^\circ$, respectively. On average, the incisive
196 foramen was located at 5.9 ± 2.3 mm below the alveolar bone crest. The mean BWs at the incisive
197 foramen level, 8 mm and 14 mm subcrestal level were 6.0 ± 1.7 mm, 6.3 ± 1.5 mm and 6.9 ± 1.9
198 mm, respectively.

199 Results of comparisons of ridge configuration between the dentulous group and the
200 edentulous group were also present in Table 2 and Fig 4. With respect to the lingual concavity, the
201 mean LCD was statistically significantly different between the dentulous group and the edentulous
202 group (1.4 ± 1.4 mm vs. 2.3 ± 1.9 mm, $p = 0.036$). In addition, the mean LCA values of the
203 dentulous group and the edentulous group were 6.6° and 10.6° respectively, which was also
204 statistically significantly different ($p = 0.022$). The distance between the incisive foramen and the
205 bone crest was closer in the edentulous group than that in the dentulous group by 1.1 mm
206 approximately ($p = 0.022$). At the incisive foramen level, the mean BW was statistically
207 significantly thinner in the edentulous group than the dentulous group by 1.2 mm approximately
208 (5.4 ± 2.5 mm vs. 6.6 ± 1.1 mm, $p = 0.013$). Furthermore, the mean BWs measured at 8 mm
209 subcrestal level of the dentulous group and the edentulous group were 6.7 mm and 5.8 mm
210 respectively, which was also statistically significantly different ($p = 0.028$). The LCH and BW

211 measured at 14 mm subcrestal level did not show statistically significant differences between the
212 two groups.

213 After 72 virtual cylindric implants (4.1×12 mm) were placed, a total of 12 sites (16.7%)
214 showed a perforation (Table 3). Three cases of them occurred in the dentulous group (8.3%) while
215 other nine cases occurred in the edentulous group (25.0%). The incidence of perforation was much
216 higher in the edentulous group, although the statistically significant difference did not exist ($p =$
217 0.058). With respect to the implant site, the incidence of perforation was statistically significantly
218 higher in the right central incisor site than in the left central incisor site (33.3% vs. 4.8%, $p =$
219 0.001). The occurrence of perforation did not show statistically significant differences between
220 genders. In the axial view images, all the perforations were located at the mesiolingual site of the
221 virtual implant. Furthermore, the depth and the area of exposure were 0.7 ± 0.6 mm (range = 0.2 -
222 2.1 mm) and 1.0 ± 1.3 mm² (range = 0.2 - 4.7 mm²), respectively. In the sagittal view images, the
223 exposure located at 8.5 ± 3.5 mm below the alveolar bone crest, with a range of 2.3 mm to 12.1
224 mm, and the length of the exposure was 5.1 ± 3.4 mm, with a range of 1.6 mm to 12.0 mm.

225 After replacing the cylindric implants with the tapered implants (4.3×13 mm), a total of 6
226 implants (8.3%) broke into the NPC, which all belonged to the edentulous group (Table 3). The
227 incidence of perforation with the selected tapered implant was statistically significantly different
228 between the dentulous and edentulous groups ($p = 0.011$). Besides, five out of six perforations
229 occurred in the right central incisor sites, and the statistically significant difference existed between
230 different sides ($p = 0.031$). The location of the exposure was at the 6.2 ± 3.2 mm below the alveolar
231 bone crest. The length, depth and area of the exposure were 5.4 ± 3.1 mm, 0.8 ± 0.6 mm and $1.3 \pm$

232 1.7 mm², respectively.

233 The numbers of perforation sites was reduced to 4 (5.6%) and 2 (2.8%) by rotating the
234 embedded direction of the cylindric implant distally by 5° and 10°, respectively. After the
235 embedded direction was rotated labially by the same degrees (5° and 10°), the incidence of
236 perforation decreased to 8.3% and 4.2%, respectively. The changes of incidences of perforation,
237 as well as the features of exposure after a minor adjustment of cylindric implant angulation, were
238 present in Table 4.

239 The multivariate logistic regression analysis revealed that the LCD was a statistically
240 significant risk factor of perforation (OR 4.332; 95% CI 1.596 – 11.760; p = 0.004). Implant
241 placement in the left central incisor site (OR 0.087; 95% CI 0.010 – 0.783; p = 0.029) and BW
242 measured at 8 mm below the alveolar bone crest (OR 0.273; 95% CI 0.111 – 0.671; p = 0.005)
243 were two protective factors appeared in the last model.

244

245 **Discussion**

246 In 2014, Chan et al. found that a buccal concavity of ridge existed anterior to the maxillary
247 central incisor.¹¹ The mean buccal concavity depth was 3.42 mm, and it was associated with the
248 occurrence of buccal plate fenestration. However, few studies have provided information regarding
249 the lingual concavity and its relationship with the NPC perforation. In the present study, all the
250 virtual implant were located at the labial-distal side of the NPC. Therefore, an obvious lingual
251 concavity, which means the NPC is located labially relatively, may increase the risk of contact of
252 implant and the neurovascular bundles in the NPC. In our study, 75% of ridges were present with

253 a lingual concavity. More importantly, the lingual concavity depth was a statistically significant
254 risk factor of NPC perforation. Therefore, not merely the incisive foramen, but also the trend of
255 the NPC direction should be carefully evaluated by CBCT to estimate whether the implant will
256 break into the interior wall of the NPC.

257 Bone dimensions anterior to the NPC is important for implant placement. In most studies, the
258 width of the bone anterior to the canal was measured at crestal, middle, and (or) the most apical
259 point of the canal in the midsagittal plane of the NPC, and the reference line was perpendicular to
260 the maxillary plane or the sagittal long axis of the canal.^{14,16} A mean bone width of 7.17 ± 1.49
261 mm has been reported in a multicenter study.¹⁴ However, the implant is rarely placed in the
262 midsagittal plane of the NPC, and also not involving the nasal part of the canal. In addition, the
263 embedded direction may be different from the direction of measurement mentioned above. As a
264 result, the data obtained by this measuring method might not reflect the implant condition
265 accurately. In this study, the bone width anterior to the NPC was first measured in the axial view
266 images at three levels: the incisive foramen level, 8 mm below the alveolar bone crestal level, and
267 14 mm below the crestal level. The incisive foramen level is where the NPC might start to hamper
268 the implant placement. The 8 mm and 14 mm below the bone crestal levels may stand for the
269 middle level and the apex level of the virtual implant selected in this study, respectively. In
270 addition, the measuring direction was perpendicular to embedded direction of implant, that is, the
271 sagittal long axis of the restoration. As a result, the measuring results of the present study may
272 reflect the real implant condition more accurately. In the present study, the mean bone width
273 anterior to the NPC was 6.0 and 6.3 mm at the incisive foramen level and 8 mm below the alveolar

274 crest level, respectively, much narrower than the bone width (7.17 mm) reported by Tözüm et al.¹⁴

275 In the present study, the incidence of NPC perforation during the maxillary central incisor
276 implant procedure was evaluated by placing a virtual implant in CBCT images. After a cylindric
277 central incisor implant (4.1 × 12 mm) was placed in the cingulum position with the long axis
278 following that of its restoration, the incidence of NPC perforation was 16.7%. In 1998, Kraut &
279 Boyden reported that the likelihood of finding a nasopalatine canal of a size that will be detrimental
280 to the placement of dental implants was approximately 4%, much lower than the likelihood present
281 in our study, by evaluating the volumes of the NPC and bone anterior to the canal in CBCT images
282 of 30 American patients.²¹ The difference of incidence was probably due to two reasons. The first
283 reason was totally different measurements. Considering that the incidence of NPC perforation is
284 associated with not only the anatomic morphology, but also the feature of implant and the three-
285 dimensional implant position, the results present in our study may reflect the clinical implant
286 condition more accurately. The second reason was different sample races. Another study of our
287 research team showed that the mean closest distance between the NPC and the apex of the central
288 incisor root were 3.88 mm in axial CBCT images (unpublished data, Jia X et al.), much closer than
289 the mean distance of 5.22 mm reported by Chatriyanuyoke et al.²⁵ The comparison of the closest
290 distances implied that insertion of implants into the NPC might be more likely to occur in Chinese
291 patients.

292 The absence of maxillary central incisors affected some dimensions and incidence of NPC
293 perforation. The results of comparison between the dentulous and edentulous group revealed that,
294 the LCD and LCA were statistically significantly greater in the edentulous group by 0.9 mm and

295 4°, respectively, although the distribution of NPC shape recorded on sagittal plane did not show
296 statistically significant differences between groups. Mardinger et al. also found that the bucco-
297 lingual NPC diameter was wider along the degree of ridge resorption.¹⁵ In the present study, it is
298 implied that a closer proximity of NPC and implant region might be present after tooth loss. In
299 addition, bone width anterior to the canal and the bone height coronal to the canal were greater in
300 dentate subjects in the present study by 1.2 mm and 1.1 mm respectively, mainly due to the alveolar
301 bone remodeling after tooth loss.^{26,27} Other studies found the same results about change of bone
302 width after tooth loss as the present study.^{14,15} Considering the ridge modeling after tooth loss,
303 including the change of LCD, LCA, BH and BW as mentioned before, it would be no surprise that
304 the incidence of NPC perforation was higher in the edentulous group than the dentulous group
305 (25.0% vs. 8.3% after cylindrical implant placement; 16.7% vs. 0.0% after taper implant placement).
306 Delayed implant placement in the maxillary central incisor site may require more care to avoid
307 NPC perforation.

308 Another interesting finding was that the perforation usually occurred in the right central
309 incisor site. The multivariate logistic regression analysis also revealed that the implant site was
310 associated with the occurrence of NPC perforation. This may be due to another finding of our
311 research team that the NPC was located on the right side at both the incisive foramen level and the
312 apex level slightly (unpublished data, Jia X et al.).

313 Regarding clinical practice, the location, length, depth, and area of perforation were described
314 in detail. In the axial view images, all the perforations were located at the mesio-lingual side of
315 the implant. However, in the sagittal view images, the perforation could occur at any part of

316 implant (2.3 – 12.1 mm below the bone crest). The mean distance between the exposure and the
317 crest was 8.5 mm in the present study, which meant that the perforation usually occurred at the
318 midroot level of the implant. In the cases of perforation, a mean length of exposure of 4.53 mm
319 predicted that the NPC perforation could not be ignored. However, on the other hand, the depth of
320 exposure was only 0.7 mm on average, which meant that a tapered implant or a minor adjustment
321 of implant angulation might be beneficial for avoiding NPC perforation.

322 The results of this study were consistent with this hypothesis. In this study, the diameter of
323 the selected tapered implant platform (4.3 × 13 mm) was a little greater than the cylindrical implant
324 by 0.2 mm, but the diameter of the tapered implant narrowed to 4.1 mm at about 3.4 mm below
325 the implant platform level, and was only 2.58 mm at the implant apex level, narrower than the
326 cylindrical implant by 1.5 mm approximately. Considering the relative shallow depth of exposure
327 after cylindrical implant placement, replacing the cylindrical implants with the tapered implants (4.3
328 × 13 mm) significantly decreased the incidence of perforation, from 16.7% to 8.3%. A minor
329 change of embedded direction was also beneficial for avoiding NPC perforation, reducing the
330 incidence to 2.8% - 4.2%. Certain considerations have to be borne in mind before the adjustment
331 of implant angulation, including the proximity of adjacent lateral incisor to the implant site and
332 the existing buccal concavity. The distance between the implant apex and the adjacent root surface
333 should not be closer than 1.5 mm after rotating the implant to the distal, while the buccal plate
334 fenestration is supposed to be avoided during rotating the implant to the labial.

335 However, neither the selected tapered implant nor a minor adjustment (less than 10°) of
336 implant angulation could avoid NPC perforation thoroughly. Therefore, it is recommended to take

337 full analysis of the NPC using CBCT at the time of implant treatment planning with consideration
338 of individual differences. The results in this study suggested that other appropriate features of
339 implant (e.g. a shorter implant or a narrower implant) or a greater embedded angle that departs
340 from the axis of the restoration might be selected to avoid perforation in some cases.

341

342 **Conclusions**

343 Within the limits of this study, it can be concluded that the NPC may get close to the implant
344 region after the central incisor extraction, and the bone width anterior to the canal may also reduce.
345 The NPC perforations may occur more commonly in edentulous patients and in the right central
346 incisor site. The right central incisor site, narrow bone width measured at 8 mm below the crest
347 and a deep lingual concavity are associated with the occurrence of NPC perforation. A minor
348 adjustment of implant angulation or a tapered implant may be beneficial for avoidance of
349 perforation.

350

351 **References**

- 352 1. Fugazzotoo PA, Vlassis J, Butler B. 2004. ITI implant use in private practice: clinical results
353 with 5,526 implants followed up to 72+ months in function. *Int J Oral Maxillofac Implants*
354 19:408-412.
- 355 2. Scheller H, Urgell JP, Kultje C, Klineberg I, Goldberg PV, Stevenson-Moore P, Alonso JM,
356 Schaller M, Corria RM, Engquist B, Toreskog S, Kastenbaum F, Smith CR. 1998. A 5-year
357 multicenter study on implant-supported single crown restorations. *Int J Oral Maxillofac*

358 *Implants* 13:212-218.

359 3. Chung WE, Rubenstein JE, Phillips KM, Raigrodski AJ. 2009. Outcomes assessment of
360 patients treated with osseointegrated dental implants at the University of Washington
361 Graduate Prosthodontic Program, 1988 to 2000. *Int J Oral Maxillofac Implants* 24:927-935.

362 4. Buser D, von Arx T. 2000. Surgical procedures in partially edentulous patients with ITI
363 implants. *Clin Oral Implants Res* 11 Suppl 1:83-100.

364 5. Garber DA, Belser UC. 1995. Restoration-driven implant placement with restoration-
365 generated site development. *Compend Contin Educ Dent* 16:796,798-802,804.

366 6. Tarnow DP, Cho SC, Wallace SS. 2000. The effect of inter-implant distance on the height of
367 inter-implant bone crest. *J Periodontol* 71:546-549.

368 7. Buser D, Martin W, Belser UC. 2004. Optimizing esthetics for implant restorations in the
369 anterior maxilla: anatomic and surgical considerations. *Int J Oral Maxillofac Implants*
370 19(Suppl.):43-61.

371 8. Grunder U, Gracis S, Capelli M. 2005. Influence of the 3-D bone-to-implant relationship on
372 esthetics. *Int J Periodontics Restorative Dent* 25:113-119.

373 9. Funato A, Salama MA, Ishikawa T, Garber DA, Salama H. 2007. Timing, positioning, and
374 sequential staging in esthetic implant therapy: a four-dimensional perspective. *Int J*
375 *Periodontics Restorative Dent* 27:313-323.

376 10. Su H, Gonzalez-Martin O, Weisgold A, Lee E. 2010. Considerations of implant abutment
377 and crown contour: critical contour and subcritical contour. *Int J Periodontics Restorative*
378 *Dent* 30:335-343.

- 379 11. Chan HL, Garaicoa-Pazmino C, Suarez F, Monje A, Benavides E, Oh TJ, Wang HL. 2014.
380 Incidence of implant buccal plate fenestration in the esthetic zone: a cone beam computed
381 tomography study. *Int J Oral Maxillofac Implants* 29:171-177.
- 382 12. Keith DA. 1979. Phenomenon of mucous retention in the incisive canal. *J Oral Surg* 37:832-
383 834.
- 384 13. Liang X, Jacobs R, Martens W, Hu Y, Adriaenssens P, Quirynen M, Lambrichts I. 2009.
385 Macro- and micro-anatomical, histological and computed tomography scan characterization
386 of the nasopalatine canal. *J Clin Periodontol* 36:598-603.
- 387 14. Tözüm TF, Güncü GN, Yıldırım YD, Yılmaz HG, Galindo-Moreno P, Velasco-Torres M,
388 Al-Hezaimi K, Al-Sadhan R, Karabulut E, Wang HL. 2012. Evaluation of maxillary incisive
389 canal characteristics related to dental implant treatment with computerized tomography: a
390 clinical multicenter study. *J Periodontol* 83:337-343.
- 391 15. Mardinger O, Namani-Sadan N, Chaushu G, Schwartz-Arad D. 2008. Morphologic changes
392 of the nasopalatine canal related to dental implantation: a radiologic study in different degrees
393 of absorbed maxillae. *J Periodontol* 79:1659-1662.
- 394 16. Bornstein MM, Balsiger R, Sendi P, von Arx T. 2011. Morphology of the nasopalatine canal
395 and dental implant surgery: a radiographic analysis of 100 consecutive patients using limited
396 cone-beam computed tomography. *Clin Oral Impl Res* 22:295-301.
- 397 17. Mraiwa N, Jacobs R, Van Cleynenbreugel J, Sanderink G, Schutyser F, Suetens P, van
398 Steenberghe D, Quirynen M. 2004. The nasopalatine canal revisited using 2D and 3D CT in
399 imaging. *Dentomaxillofac Radiol* 33:396-402.

- 400 18. Casado PL, Donner M, Pascarelli B, Derocy C, Duarte ME, Barboza EP. 2008. Immediate
401 dental implant failure associated with nasopalatine duct cyst. *Implant Dent* 17:169-175.
- 402 19. Takeshita K, Funaki K, Jimbo R, Takahashi T. 2013. Nasopalatine duct cyst developed in
403 association with dental implant treatment: A case report and histopathological observation. *J*
404 *Oral Maxillofac Pathol* 17:319.
- 405 20. McCrea SJ. 2014. Nasopalatine duct cyst, a delayed complication to successful dental
406 implant placement: diagnosis and surgical management. *J Oral Implantol* 40:189-195.
- 407 21. Kraut RA, Boyden DK. 1998. Location of incisive canal in relation to central incisor implants.
408 *Implant Dent* 7:221-225.
- 409 22. White SC. 2008. Cone-beam imaging in dentistry. *Health Phys* 95:628-637.
- 410 23. Fortin T, Bosson JL, Coudert JL, Isidori M. 2003. Reliability of preoperative planning of an
411 image-guided system for oral implant placement based on 3-dimensional images: An in vivo
412 study. *Int J Oral Maxillofac Implants* 18:886-893.
- 413 24. Katsoulis J, Pazera P, Mericske-Stern R. 2009. Prosthetically driven, computer-guided
414 implant planning for the edentulous maxilla: A model study. *Clin Implant Dent Relat*
415 *Res* 11:238-245.
- 416 25. Chatriyanuyoke P, Lu CI, Suzuki Y, Lozada JL, Rungcharassaeng K, Kan JY, Goodacre CJ.
417 2012. Nasopalatine canal position relative to the maxillary central incisors: a cone beam
418 computed tomography assessment. *J Oral Implantol* 38:713-717.
- 419 26. Araújo MG, Lindhe J. 2005. Dimensional ridge alterations following tooth extraction. An
420 experimental study in the dog. *J Clin Periodontol* 32:212-218.

421 27. Schropp L, Wenzel A, Kostopoulos L, Karring T. 2003. Bone healing and soft tissue contour
422 changes following single-tooth extraction: a clinical and radiographic 12-month prospective
423 study. *Int J Periodontics Restorative Dent* 23:313-323.
424

425

Table 1 General characteristics of 72 subjects included in the study

	Total (n=72)	Dentulous group (n=36)	edentulous group (n=36)	p value
Age (mean \pm SD)	45.6 \pm 8.8	45.5 \pm 9.0	45.6 \pm 8.8	0.906
Gender (n)				
male	54	27	27	
female	18	9	9	1.000
Implant site (n)				
Right central incisor	30	15	15	
Left central incisor	42	21	21	1.000
Canal shapes (n)				
cylindrical	29	17	12	
funnel-like	17	6	11	
hourglass-like	15	9	6	
banana-like	11	4	7	0.290

426

427

428

Table 2 Ridge configuration and comparison results according to dental status (mean \pm SD)

Variable	Total (n=72)	Dentulous group (n=36)	Edentulous group (n=36)	p value
Lingual Concavity				
LCD (mm)	1.8 \pm 1.7	1.4 \pm 1.4	2.3 \pm 1.9	0.036
LCH (mm)	14.3 \pm 7.3	13.9 \pm 7.8	14.8 \pm 6.8	0.539
LCA ($^{\circ}$)	8.6 \pm 6.5	6.6 \pm 5.9	10.6 \pm 6.5	0.022
BH (mm)	5.9 \pm 2.3	6.5 \pm 1.9	5.4 \pm 2.5	0.022
BW (mm)				
incisive foramen level	6.0 \pm 1.7	6.6 \pm 1.1	5.4 \pm 2.0	0.013
8 mm subcrestal level	6.3 \pm 1.5	6.7 \pm 1.2	5.8 \pm 1.6	0.028
14 mm subcrestal level	6.9 \pm 1.9	7.0 \pm 1.6	6.7 \pm 2.1	0.401

429 LCD: lingual concavity depth; LCH: lingual concavity height; LCA: lingual concavity angulation; BH: bone

430 height coronal to the canal; BW: bone width anterior to the canal

431

432

Table 3 Frequency distribution of perforation with different implant type

Group	Implants (number)	Number of Perforations (number and percent)	
		Cylindric 4.1 × 12 mm	Tapered 4.3 × 13 mm
Dental Status			
dentulous group	36	3 (8.3%)	0 (0.0%)**
edentulous group	36	9 (25.0%)	6 (16.7%)**
Implant Site			
right central incisor site	30	10 (33.3%)*	5 (16.7%)***
left central incisor site	42	2 (4.8%)*	1 (2.4%)***
Gender			
male	54	7 (13.0%)	3 (5.6%)
female	18	5 (27.8%)	3 (16.7%)
Total	72	12 (16.7%)	6 (8.3%)

433 * Statistically significant difference exists between implant sites with cylindric implant ($p = 0.001$).

434 ** Statistically significant difference exists between dentulous and edentulous groups with tapered implant ($p =$
435 0.011).

436 *** Statistically significant difference exists between implant sites with tapered implant ($p = 0.031$).

437

438

Table 4 Change of perforation after a minor adjustment of implant angulation

Embedded Direction	Number (Percent)	Location (mm)	Length (mm)	Depth (mm)	Area (mm ²)
Axis of Restoration	12 (16.7%)	8.5 ± 3.5	5.1 ± 3.4	0.7 ± 0.6	1.0 ± 1.3
Distal by 5°	4 (5.6%)	5.4 ± 3.7	5.5 ± 2.0	0.8 ± 0.4	3.9 ± 4.9
Distal by 10°	2 (2.8%)	2.4 ± 0.1	6.6 ± 2.1	1.1 ± 0.2	2.3 ± 0.7
Labial by 5°	6 (8.3%)	6.8 ± 3.7	5.9 ± 3.9	0.9 ± 0.7	1.5 ± 1.9
Labial by 10°	3 (4.2%)	5.3 ± 4.9	8.2 ± 5.1	1.2 ± 0.9	2.4 ± 2.4

439

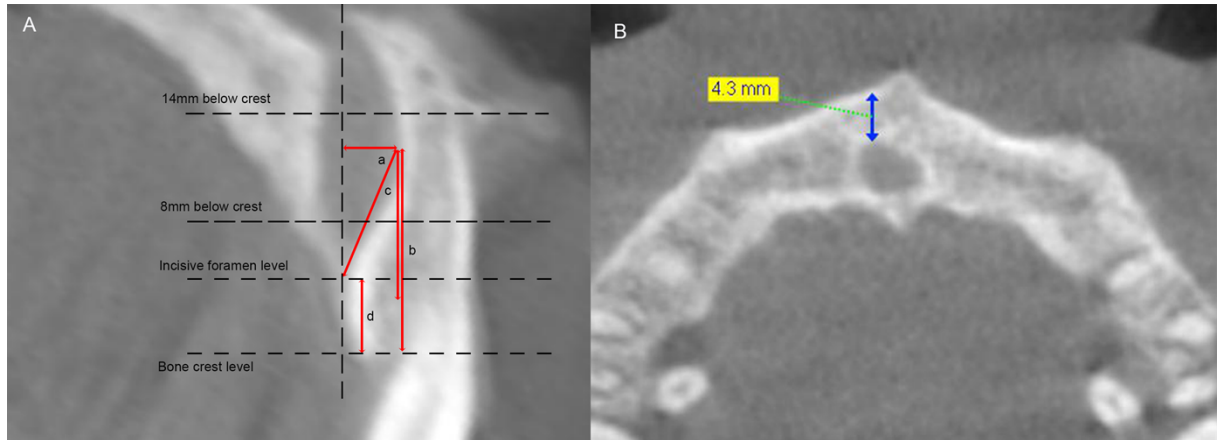
440

Table 5 Multivariate logistic regression of factors affecting the NPC perforation

Variables	β	OR	95% CI	P Value
Left central incisor site	-2.446	0.087	0.010 - 0.783	0.029
BW measured at 8 mm below crest	-1.299	0.273	0.111 - 0.671	0.005
LCD	1.466	4.332	1.596 - 11.760	0.004
Constant	1.974	7.200		0.329

441 NPC: nasopalatine canal; BW: bone weight anterior to the canal; LCD: lingual concavity depth.

442



443

444 Figure 1 Configuration of Ridge Anterior to the NPC. A, a = the lingual concavity depth (LCD);

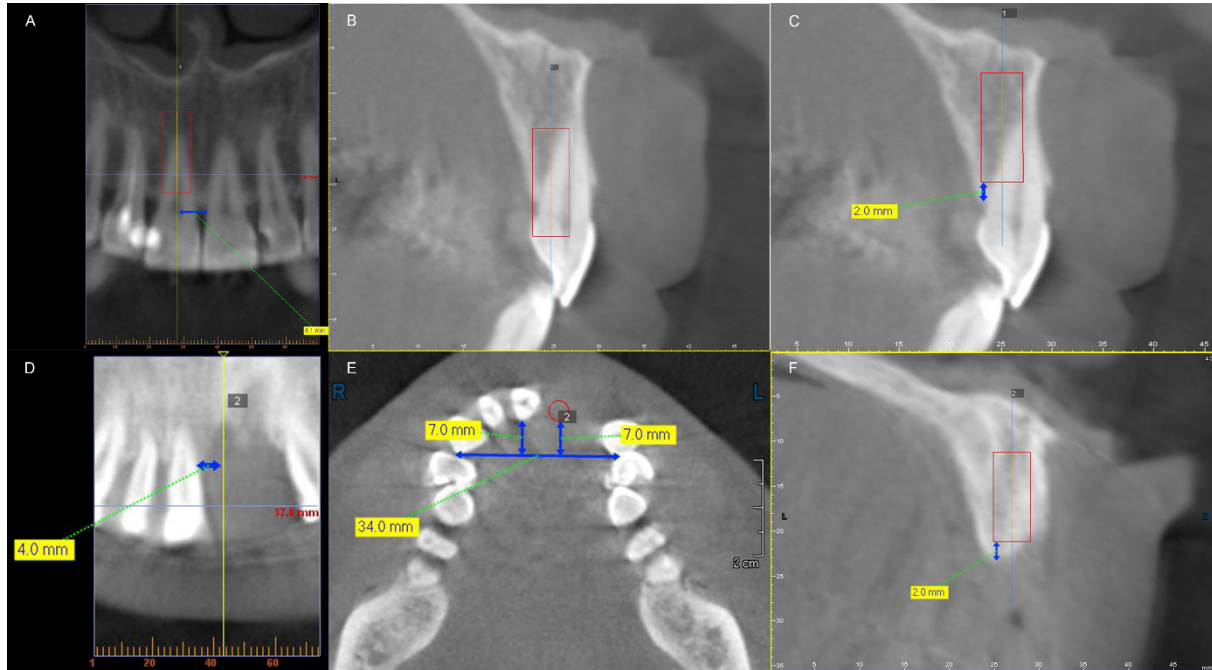
445 b = the lingual concavity height (LCH); c = the lingual concavity angulation (LCA); d = the

446 height of the alveolar bone coronal to the NPC (BH). B, the arrow stands for minimum bone

447 width anterior to the NPC (BW), measured at incisive foramen level, 8 mm and 14 mm below

448 bone crest level, respectively.

449



450

451 Figure 2 three-dimensional location of virtual implant in dentulous patients (A, B, C) and

452

edentulous patients (D, E, F). A and D, mesiodistal location in dentulous and edentulous

453

group; B and E, buccolingually, the implant platform was placed at the cingulum of the

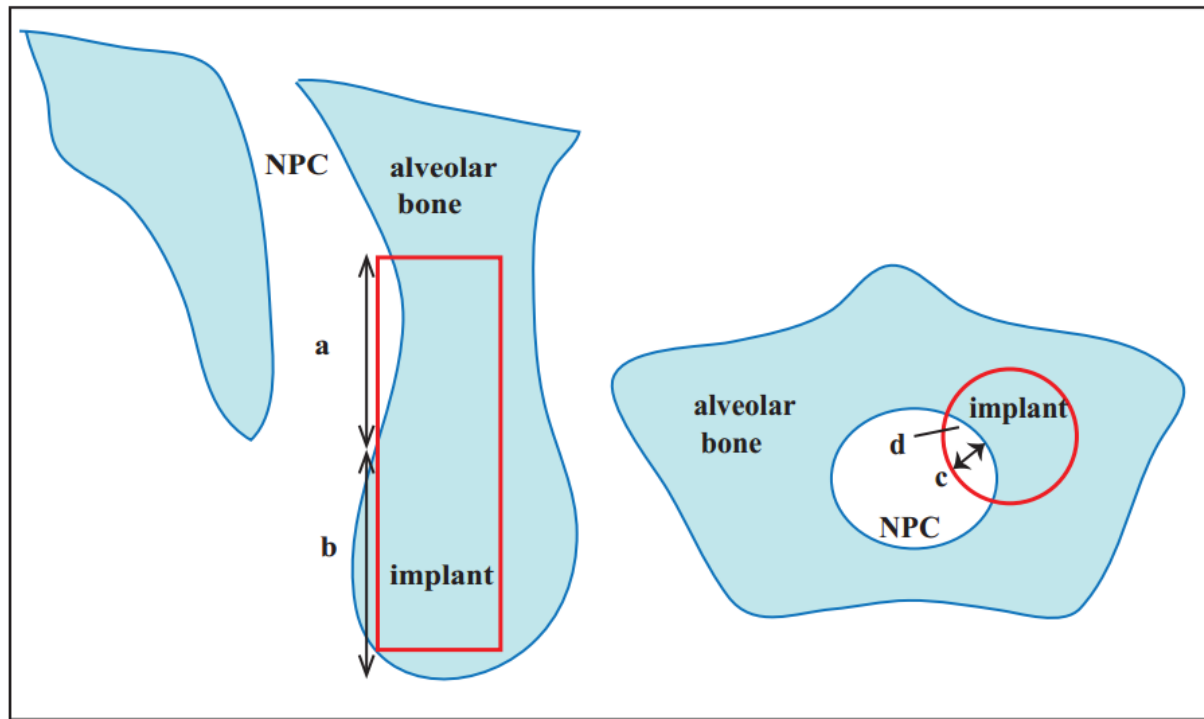
454

future restoration in both dentulous and edentulous group; C and F, apicocoronally, the

455

implant platform was located 2 mm below the alveolar bone crest in both groups.

456



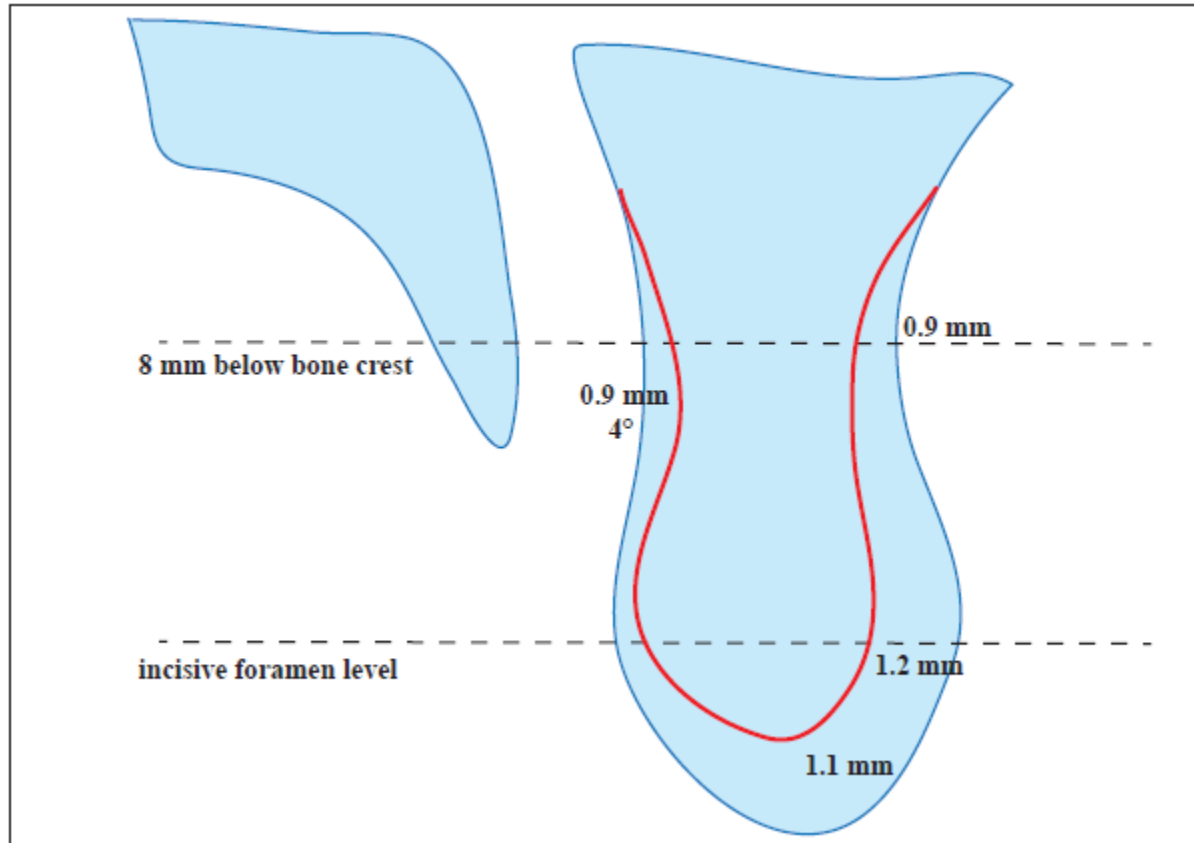
457

458 Figure 3 Description of nasopalatine canal (NPC) perforation in both sagittal slice and axial slice.

459 a = length of exposure; b = distance between the alveolar crest and the perforation

460 (location of perforation); c = the depth of the exposure; d = the area of the exposure.

461



462

463 Figure 4 Comparison of ridge configuration anterior to the NPC between dentulous and edentulous

464 patients. The red line stands for the ridge contour of edentulous patients.